

Landau-Zener dynamics of a nanoresonator containing a tunneling spin

Michael F. O’Keeffe, Eugene M. Chudnovsky, and Dmitry A. Garanin
*Physics Department, Lehman College, City University of New York,
 250 Bedford Park Boulevard West, Bronx, New York, 10468-1589, USA*
 (Dated: February 26, 2013)

We study the Landau-Zener dynamics of a tunneling spin coupled to a torsional resonator. For strong spin-phonon coupling, when the oscillator frequency is large compared to the tunnel splitting, the system exhibits multiple Landau-Zener transitions. Entanglement of spin and mechanical angular momentum results in abrupt changes of oscillator dynamics which coincide in time with spin transitions. We show that a large number of spins on a single oscillator coupled only through the in-phase phonon field behaves as a single large spin, greatly enhancing the spin-phonon coupling. We compare purely quantum and semiclassical dynamics of the system and discuss their experimental realizations. An experiment is proposed in which the field sweep is used to read out the exact quantum state of the mechanical resonator.

PACS numbers: 75.80.+q, 75.45.+j, 75.50.Xx, 85.65.+h

I. INTRODUCTION

The Landau-Zener model¹ describes a two-state system in which the bias between diagonal states varies linearly with time as they are swept through an avoided crossing. It is one of the few practically important time-dependent Hamiltonians for which the Schrödinger equation is exactly solvable. The Landau-Zener method has recently found a natural application in the experimental characterization of single molecule magnets². Theoretical studies of Landau-Zener transitions in nanomagnets have included many-body effects³ and superradiance⁴. Some important theorems have been proven about generalizations of the Landau-Zener problem⁵, and certain multi-level cases have been exactly solved⁶. It has been used as a model for the dynamics of quantum phase transitions⁷, and topological defect formation⁸.

A natural extension of the two-level quantum physics is the two-level system coupled to one or several quantized modes of a harmonic oscillator. Studies of Landau-Zener oscillator dynamics have probed coherent^{9,10}, dissipative^{11,12}, and temperature-dependent¹³ effects. Landau-Zener interferometry has provided a quantitative measure of coupled dynamics¹⁴ and has been experimentally verified in the nanomechanical measurement of a superconducting qubit¹⁵.

The Landau-Zener effect in spin systems should be considered in conjunction with the transfer of angular momentum manifested in the Einstein - de Haas effect. This effect has allowed precision measurement of the magneto-mechanical ratio of a thin ferromagnetic film on a microcantilever¹⁶. Torsional oscillators have been used as precision torque magnetometers in nanomechanical detection of itinerant electron spin-flip at a ferromagnet-normal metal junction¹⁷ and measurement of phase transitions of small magnetic disks in and out of the vortex state¹⁸. Semiclassical models of Landau-Zener dynamics have been developed to describe magnetic molecules coupled to mechanical resonators and bridged between conducting leads^{19,20}. A full quantum treatment of the

interaction between a single spin and a torsional oscillator has recently been developed^{21,22}.

Realizing a quantum magneto-mechanical system with strong spin-phonon coupling has been an experimental challenge. A recent experiment²³ has shown the first evidence of strong spin-phonon coupling in a single molecule magnet grafted onto a carbon nanotube. Spin reversal of the single molecule magnet during a Landau-Zener sweep coincides with an abrupt increase in the differential conductance through the carbon nanotube. This has been interpreted as the spin transition exciting a longitudinal stretching mode of the carbon nanotube, which enhances electron tunneling from the lead onto the nanotube through electron-phonon coupling.

We propose multiple schemes to realize strongly coupled dynamics of a tunneling macrospin with torsional oscillations of a nanoresonator in a Landau-Zener experiment. We investigate the Landau-Zener dynamics of a tunneling spin coupled to a torsional oscillator, using a fully quantum mechanical model. The oscillator could be a torsional paddle resonator, a microcantilever, a carbon nanotube, or a single magnetic molecule between two point contacts. The tunneling spin could be a single molecule magnet, an ensemble of single molecule magnets, or a single-domain ferromagnetic particle with strong uniaxial anisotropy. For a collection of single molecule magnets placed on a torsional resonator or cantilever far apart from each other that they are not directly coupled through dipole interactions, we develop a semiclassical model of magnetization dynamics. We predict superradiant enhancement⁴ of the spin-phonon coupling for this ensemble system. Comparison of these two models shows their correspondence.

The coupling between spin and mechanical angular momentum is mandated by the conservation of total angular momentum $\mathbf{J} = \mathbf{S} + \mathbf{L}$, with \mathbf{L} being the mechanical angular momentum. In a free particle, when a spin tunnels from \mathbf{S} to $-\mathbf{S}$, the particle must change its mechanical angular momentum \mathbf{L} . This changes its kinetic energy by an amount of order $\hbar^2 \mathbf{S}^2 / I$, where I_z is the

moment of inertia about the rotation axis. For a macroscopically large body, the large moment of inertia makes this rotational kinetic energy negligibly small. But for a small particle this can become comparable to the energy gain Δ due to tunnel splitting²⁴. The ratio of these two quantities, the magneto-mechanical ratio $\alpha = 2\hbar^2 S^2 / I_z \Delta$ determines the ground state of the system for a free particle²⁵. For large particles $\alpha \ll 1$ and the ground state is the well-known tunnel split state $\Psi \sim |\psi_S\rangle + |\psi_{-S}\rangle$. For small particles, such as the Fe₈ single molecule magnet with $I_z \sim 10^{-42}$ kg·m², $\alpha \gg 1$ and spin tunneling is suppressed as the spin localizes in either direction along the easy axis.

Similar effects arise in systems that undergo torsional oscillations. Examples are a single molecule magnet bridged between conducting leads, a nanomagnet attached to a carbon nanotube bridge, or a nanomagnet coupled to a resonator such as a torsional paddle oscillator or microcantilever. The mechanical resonance occurs at a frequency $\omega_r = \sqrt{k/I_z}$, where k is the effective stiffness against the linear restoring torque and I_z is the moment of inertia of the nanomagnet-resonator combination. A convenient measure of the effect of oscillations is the dimensionless parameter $r = \hbar\omega_r/\Delta$, the ratio between the oscillator energy to tunnel splitting. As we will see in Sec. II, the coupling between magnetization and oscillator dynamics is given by the factor $\lambda = \sqrt{\alpha}/r = \sqrt{2\hbar S^2/I_z \omega_r}$. The most interesting effects occur for strong coupling $\lambda \sim 1$ and oscillator frequency much larger than tunnel splitting $r \gg 1$. A large spin, small moment of inertia, and weak torsional spring constant are required for strong coupling. article is organized

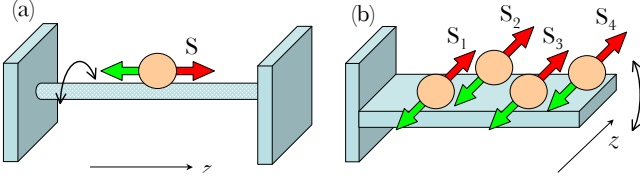


FIG. 1. Possible experimental geometries described by the models studied in this paper. In both cases the easy axis of the macrospin coincides with the rotation axis of the oscillator. (a) Single molecule magnet grafted on a carbon nanotube. (b) Ensemble of single molecule magnets on a nanocantilever.

as follows. In Sec. II we briefly review the Landau-Zener model, and construct the quantum mechanical model of a spin coupled to a torsional resonator with an external magnetic field that varies linearly in time. Sec. III contains numerical and analytical results of the fully quantum spin dynamics for a variety of parameter ranges. Oscillator dynamics are presented in Sec. IV. A semi-classical model of superradiant dynamics in an ensemble of spins on a single resonator is developed in Sec. V. Finally, we discuss the interpretation of our results for various experimental realizations in Sec. VI.

II. MODEL

A. Landau-Zener Transitions in a Two-State System

We review relevant features of the Landau-Zener model, which describes a two-level system driven by a classical field that varies linearly in time. The LZ Hamiltonian is

$$\hat{H}_{LZ} = -\frac{vt}{2}\sigma_z - \frac{\Delta}{2}\sigma_x, \quad (1)$$

in terms of Pauli matrices σ_z and $\sigma_x = \sigma_+ + \sigma_-$, where v is the sweep rate and Δ is the tunnel splitting. Diabatic states $|\uparrow\rangle$ and $|\downarrow\rangle$ are eigenstates of σ_z with diabatic energies $E_{\uparrow\downarrow}(t) = \pm vt/2$, which are the linear functions in Fig. 2a. We take the sweep rate v positive, so the positive (negative) sign corresponds to spin down (up). For nonzero Δ , the diabatic states are not eigenstates of the Hamiltonian. Diagonalizing \hat{H}_{LZ} gives adiabatic energies

$$E_{\pm}(t) = \pm \frac{1}{2} \sqrt{(vt)^2 + \Delta^2} \quad (2)$$

which are the upper and lower curves in Fig. 2a with splitting Δ at $t = 0$. The corresponding adiabatic eigenstates $|\pm\rangle$ and $|\mp\rangle$ are

$$|\pm\rangle = \frac{1}{\sqrt{2}}(C_{\mp}|\uparrow\rangle \mp C_{\pm}|\downarrow\rangle), \quad (3)$$

where C_{\pm} depend explicitly on time,

$$C_{\pm} = \sqrt{1 \pm \frac{vt}{\sqrt{(vt)^2 + \Delta^2}}}. \quad (4)$$

For times $|t| \gg \Delta/v$ the adiabatic states asymptotically coincide with the diabatic states.

The state of the system

$$\Psi(t) = c_{\uparrow}(t)|\uparrow\rangle + c_{\downarrow}(t)|\downarrow\rangle \quad (5)$$

evolves according to the time-dependent Schrödinger equation

$$i\hbar \frac{\partial \Psi}{\partial t} = \hat{H} \Psi \quad (6)$$

with initial conditions $c_{\uparrow}(-\infty) = 0$, $|c_{\downarrow}(-\infty)| = 1$. After eliminating c_{\downarrow} , we obtain the second order differential equation

$$\ddot{c}_{\uparrow}(t) + \left[\left(\frac{\Delta}{2\hbar} \right)^2 - \frac{iv}{2\hbar} + \left(\frac{vt}{2\hbar} \right) \right] c_{\uparrow}(t) = 0 \quad (7)$$

which can be put into the standard form of the Weber equation. The exact solution¹ gives

$$c_{\uparrow}(t) = \sqrt{\gamma} e^{-\pi\gamma/4} D_{-\nu-1}(-iz) \quad (8)$$

where

$$\gamma = \frac{\Delta^2}{4\hbar v}, \quad \nu = i\gamma, \quad z = \sqrt{\frac{v}{\hbar}} e^{-i\pi/4} t, \quad (9)$$

and $D_{-\nu-1}(-iz)$ are parabolic cylinder functions. The staying probability for the spin-down state as function of time is $P(t) = |c_{\downarrow}(t)|^2$. The exact asymptotic limit for $t = \infty$, known as the Landau-Zener probability, is

$$P_{LZ} = e^{-\epsilon}, \quad \epsilon = \frac{\pi\Delta^2}{2\hbar v}. \quad (10)$$

$P(t)$ and P_{LZ} are shown in Fig. 2b. The same $P(t)$ and P_{LZ} can be obtained from the Heisenberg equations of motion for $\langle\sigma_z(t)\rangle$. An intuitive understanding

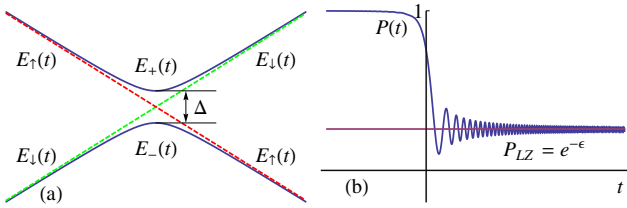


FIG. 2. (a) Adiabatic $E_{\pm}(t)$ and diabatic $E_{\uparrow\downarrow}(t)$ energy levels of the LZ Hamiltonian as a function of time. (b) Probability $P(t)$ of staying in the initial $|\downarrow\rangle$ state as a function of time, and asymptotic staying probability P_{LZ} .

of the Landau-Zener transition comes from considering the time spent in the tunneling region between adiabatic states and the tunneling time between these states. Let $\tau_{LZ} \sim \max(\sqrt{\hbar/v}, \Delta/v)$ be the time spent in the tunneling region and $\tau_{\Delta} \sim \hbar/\Delta$ be the tunneling time at the crossing. The Landau-Zener exponent is proportional to the ratio of these times $\epsilon \sim \tau_{LZ}/\tau_{\Delta}$. For a slow sweep the system will evolve adiabatically, spending long enough in the tunneling region that it will continually relax to the ground state, making $\epsilon \gg 1$ and $P_{LZ} \rightarrow 0$. In the opposite limit, a fast sweep through the tunneling region makes $\epsilon \ll 1$ and the staying probability saturates at $P_{LZ} \rightarrow 1$.

B. Landau-Zener Transitions in a Spin-Oscillator System

Consider a tunneling spin which is projected onto the lowest tunneling doublet. This spin is coupled to a torsional nanoresonator with rigidity k that can rotate about the z -axis, which coincides with the easy axis of the spin. The Hamiltonian is^{21,22},

$$\hat{H} = \frac{\hbar^2 L_z^2}{2I} + \frac{I_z \omega_r^2 \phi^2}{2} - \frac{W(t)}{2} \sigma_z - \frac{\Delta}{2} (e^{-i2S\phi} \sigma_+ + e^{i2S\phi} \sigma_-). \quad (11)$$

The fundamental frequency of torsional oscillations is $\omega_r = \sqrt{k/I_z}$, where I_z is the moment of inertia of the

resonator about its rotation axis. An external longitudinal magnetic field $B_z(t)$ applied along this axis creates a time-dependent energy bias $W(t) = 2Sg\mu_B B_z(t)$. The Landau-Zener problem describes a linear field sweep, $W(t) = vt$. The operator of mechanical angular momentum, $L_z = -i\partial_\phi$, and the angular displacement ϕ of the oscillator obey the usual commutation relation $[\phi, L_z] = i$.

The last term in the Hamiltonian describes the entanglement between spin transitions and mechanical rotations. A typical single molecule magnet has a large spin and strong uniaxial anisotropy, producing a zero-field splitting between degenerate ground states $|\psi_{\pm S}\rangle$ pointing in either direction along the easy axis. Any symmetry breaking interactions, such as transverse anisotropy or an external field, break this degeneracy producing tunnel split states $\Psi \sim |\psi_S\rangle \pm |\psi_{-S}\rangle$ which are represented by the pseudospin σ . The tunnel splitting Δ is generally many orders of magnitude less than the energy to the next spin level. In the case of the spin-10 single molecule magnet Fe_8 , the crystal field Hamiltonian describing the magnetic anisotropy is $\hat{H}_S = -D\hat{S}_z^2 + d\hat{S}_y^2$, with $d \ll D$. Full perturbation theory²⁶ gives

$$\Delta = \frac{8S^{3/2}}{\pi^{1/2}} \left(\frac{d}{4D} \right)^S D, \quad (12)$$

where we can see that $\Delta \ll 2SD$, which is the distance to the next spin level. The crystal field Hamiltonian \hat{H}_S is defined with respect to coordinate axes that are rigidly coupled to the molecule or crystal. Because the particle is free to rotate, the crystal field Hamiltonian must be transformed to the fixed frame of the laboratory. Projecting the crystal field Hamiltonian onto the lowest tunneling doublet, rotating to the lab frame using $\hat{U}(\hat{S}_z) = e^{i\hat{S}_z\phi}$, where $\hat{S}_z|\psi_{\pm S}\rangle \simeq \pm S|\psi_{\pm S}\rangle$, $\hat{H}'_S = \hat{U}\hat{H}_S\hat{U}^{-1}$ gives the final term of the Hamiltonian.

We now consider the spin-oscillator Hamiltonian with a linear field sweep $W(t) = vt$. Introducing the usual annihilation and creation operators, a and a^\dagger ,

$$\phi = \sqrt{\frac{\hbar}{2I_z\omega_r}} (a^\dagger + a), \quad L_z = i\sqrt{\frac{I_z\omega_r}{2\hbar}} (a^\dagger - a) \quad (13)$$

into Eq. (11) gives

$$\hat{H} = \hbar\omega_r a^\dagger a - \frac{vt}{2} \sigma_z - \frac{\Delta}{2} (e^{-i\lambda(a^\dagger+a)} \sigma_+ + e^{i\lambda(a^\dagger+a)} \sigma_-), \quad (14)$$

where we have dropped unessential constant terms. We will find it useful to adopt dimensionless units $\hat{H}' = \hat{H}/\Delta$ and $t' = \Delta t/\hbar$,

$$\hat{H}' = r a^\dagger a - \frac{v't'}{2} \sigma_z - \frac{1}{2} (e^{-i\lambda(a^\dagger+a)} \sigma_+ + e^{i\lambda(a^\dagger+a)} \sigma_-), \quad (15)$$

which shows that the system depends on three parameters. The parameters

$$\lambda = \sqrt{\frac{2\hbar S^2}{I_z\omega_r}}, \quad r = \frac{\hbar\omega_r}{\Delta} \quad (16)$$

describe the spin-oscillator relationship. λ is the coupling strength between the spin and oscillator and r is the ratio of mechanical oscillation to tunnel splitting frequency. The relationship between λ and r can be understood by the so-called magneto-mechanical ratio,

$$\alpha = \lambda^2 r = \frac{2\hbar^2 S^2}{I_z \Delta}, \quad (17)$$

which is the ratio of the change in rotational kinetic energy associated with a spin transition $\mathbf{S} \rightarrow -\mathbf{S}$ to the tunnel splitting energy. The third parameter is the effective sweep rate v' , or equivalently the Landau-Zener exponent ϵ defined in Eq. (10),

$$v' = \frac{\pi}{2\epsilon} = \frac{\hbar v}{\Delta^2}. \quad (18)$$

We choose the spin up/down basis for the two-level system and a Fock state basis for the harmonic oscillator. A direct product of these two bases will form the basis of the spin-oscillator system. Matrix elements of the Hamiltonian Eq. (14) are

$$H_{m\sigma, n\sigma'} = \left(\hbar\omega_r m - \frac{vt}{2} \sigma \right) \delta_{mn} \delta_{\sigma\sigma'} - \left[\frac{\Delta_{mn}}{2} \delta_{\sigma, -1} \delta_{\sigma', 1} + \frac{\Delta_{mn}^*}{2} \delta_{\sigma, 1} \delta_{\sigma', -1} \right], \quad (19)$$

where $\sigma = -1, 1$ corresponds to spin down and up states, respectively. The full Fock space has an infinite number of states, although we will use a truncated basis for numerical computations. Tunneling matrix elements

$$\Delta_{mn} = \Delta \kappa_{mn}(\lambda), \quad (20)$$

depend on the coupling λ through matrix elements of the displacement operator $\hat{D}(\xi) = \exp(\xi a^\dagger - \xi^* a)$, $\xi = -i\lambda$,

$$\kappa_{mn}(\lambda) = e^{-\lambda^2/2} (-i\lambda)^{m-n} \sqrt{\frac{n!}{m!}} L_n^{(m-n)}(\lambda^2) \quad (21)$$

for $m \geq n$, and $m \leq n$ for $m < n$. $L_n^{(m-n)}(x)$ are generalized Laguerre polynomials, and the real parameter λ is defined in Eq. (16). The first few κ_{mn} are

$$\begin{aligned} \kappa_{00} &= e^{-\lambda^2/2}, & \kappa_{01} &= \kappa_{10} = -i\lambda e^{-\lambda^2/2}, \\ \kappa_{11} &= (1 - \lambda^2) e^{-\lambda^2/2}. \end{aligned} \quad (22)$$

III. LANDAU-ZENER SPIN-OSCILLATOR DYNAMICS

A. Adiabatic energy levels

Numerically solving $\det(\hat{H} - EI) = 0$ gives the adiabatic energy levels $E_{n\pm}$, shown in Fig. 3. Diabatic energy

levels $E_{n\downarrow\uparrow}$, dotted lines in the insets of Fig. 3, are eigenvalues of the noninteracting part of the Hamiltonian (the first two terms in Eq. (14)), given by

$$\frac{E_{n\downarrow\uparrow}}{\Delta} = nr \pm \frac{v't'}{2}. \quad (23)$$

The spin down (up) states have positive (negative) slopes with y -intercepts $n\omega$. Diabatic energies $E_{n\downarrow}$ and $E_{m\uparrow}$ cross at times

$$t'_k = k \frac{r}{v'}, \quad k = m - n \in \mathbb{Z}. \quad (24)$$

When the oscillator frequency is much larger than the

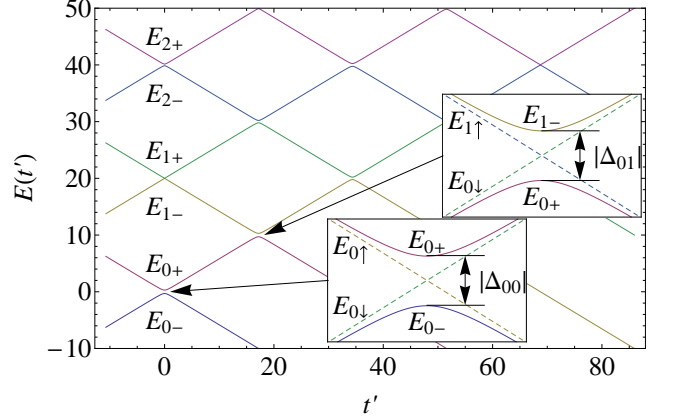


FIG. 3. Energy (in units of Δ) as a function of time for $r = 20$, $\lambda = 1$, $\epsilon = 1.35$. Solid lines are adiabatic energy levels $E_{n\pm}$, and diabatic energies $E_{n\downarrow\uparrow}$ are dashed lines in the insets. Crossings occur at t_k .

sweep rate, $r \gg v'$, the transitions are independent. Note that the indices on the adiabatic and diabatic energies only coincide near $t = 0$, but will in general be different after successive crossings. The tunnel splittings $|\Delta_{mn}|$ between adiabatic states occur at the crossing of diabatic energies $E_{m\downarrow}$ and $E_{n\uparrow}$, and depend on the coupling strength through Eqs. (20) and (21). When $r \gtrsim v'$, successive transitions occur within short times of each other. Once $r \lesssim v'$ there are many closely spaced levels near $t = 0$.

Consider a single spin initially spin-down with the oscillator in the zero phonon state, i.e. $\Psi(t = -\infty) = |0\rangle \downarrow$. The system is initially in the adiabatic energy state E_{0-} which corresponds to the diabatic state $E_{0\downarrow}$. At $t_0 = 0$, diabatic states $E_{0\downarrow}$ and $E_{0\uparrow}$ cross, and adiabatic states E_{0-} and E_{0+} approach each other with minimum separation $|\Delta_{00}| = \Delta e^{-\lambda^2/2}$. If the spin remains in the initial adiabatic state E_{0-} after the avoided crossing, it flips and will see no more possible transitions, as E_{0-} coincides with $E_{0\uparrow}$ long after the avoided crossing at t_0 . If the spin does not flip, it will follow the adiabatic state E_{0+} which coincides with $E_{0\downarrow}$ long after t_0 . The next crossing between diabatic states $E_{0\downarrow}$ and $E_{1\uparrow}$ occurs at t_1 , with tunnel splitting $|\Delta_{01}| = \Delta e^{-\lambda^2/2} \lambda$ between adiabatic states E_{0+} and E_{1-} . Remaining in the adiabatic

state E_{0+} will coincide with $E_{1\uparrow}$ for times long after t_1 . If the spin does not flip at t_1 , the system will remain in the E_{1-} adiabatic state, coinciding with $E_{0\downarrow}$ long after t_1 . In general the crossing between state $|0\rangle|\downarrow\rangle$ and $|k\rangle|\uparrow\rangle$ occurs at t_k with splitting $|\Delta_{0k}| = \Delta e^{-\lambda^2/2} |\kappa_{0k}(\lambda)|$. Notice that the avoided crossing between E_{1-} and E_{1+} at $t_0 = 0$, given by $|\Delta_{11}| = \Delta e^{-\lambda^2/2} |1 - \lambda^2|$ does exactly go to zero when $\lambda = 1$.

B. Strong coupling

We study the dynamics of the spin-oscillator system for various parameter ranges. Expanding the wave function of the system in this basis

$$|\Psi(t)\rangle = \sum_{m=0}^{\infty} \sum_{\sigma=\pm 1} C_{m\sigma}(t) |m\rangle |\sigma\rangle, \quad (25)$$

the time-dependent Schrödinger equation yields the system of coupled differential equations,

$$i \frac{dC_{m,\sigma}}{dt'} = \left(rm - \frac{v't'}{2} \sigma \right) C_{m,\sigma} - \sum_{n,\sigma'} \left[\frac{\kappa_{mn}}{2} \delta_{\sigma,-1} \delta_{\sigma',1} + \frac{\kappa_{mn}^*}{2} \delta_{\sigma,1} \delta_{\sigma',-1} \right] C_{n,\sigma'}. \quad (26)$$

We solve this system of equations numerically with a truncated oscillator basis. First we consider the initial state of the spin system to be spin-down with the oscillator in its quantum ground state $|\Psi(-\infty)\rangle = |0\rangle|\downarrow\rangle$, which gives $C_{0,-1}(-\infty) = 1$ with all other $C_{m,\sigma}(-\infty) = 0$.

Strong coupling ($\lambda \sim 1$) of spin dynamics to torsional oscillations results in rich dynamics of both the spin and the oscillator. Calculating the expectation value of σ_z ,

$$\langle \sigma_z \rangle = \sum_{m,\sigma} \sigma |C_{m,\sigma}|^2 \quad (27)$$

we define the probability of staying in the initial spin-down state as

$$P(t) = \frac{1}{2} (1 - \langle \sigma_z \rangle). \quad (28)$$

A comparison of staying probabilities for different parameters is shown in Fig. 4. For $r \gg 1$, the spin transitions are clearly independent, as shown in Figs. 4a and 4b. The tunnel splitting at each crossing is strongly renormalized, according to Eq. (20), which leads to strong dependence of the transition probability on the coupling.

Consider the crossing of diabatic energies $E_{m\downarrow}$ and $E_{n\uparrow}$. For the system initially in the $|m\rangle|\downarrow\rangle$ state, which corresponds to the lower of the two adiabatic states long before the avoided crossing, the probability that the system will stay in the initial state is

$$P_{mn} = e^{-\epsilon_{mn}}, \quad \epsilon_{mn} = \frac{\pi \Delta^2 |\kappa_{mn}|^2}{2\hbar v}. \quad (29)$$

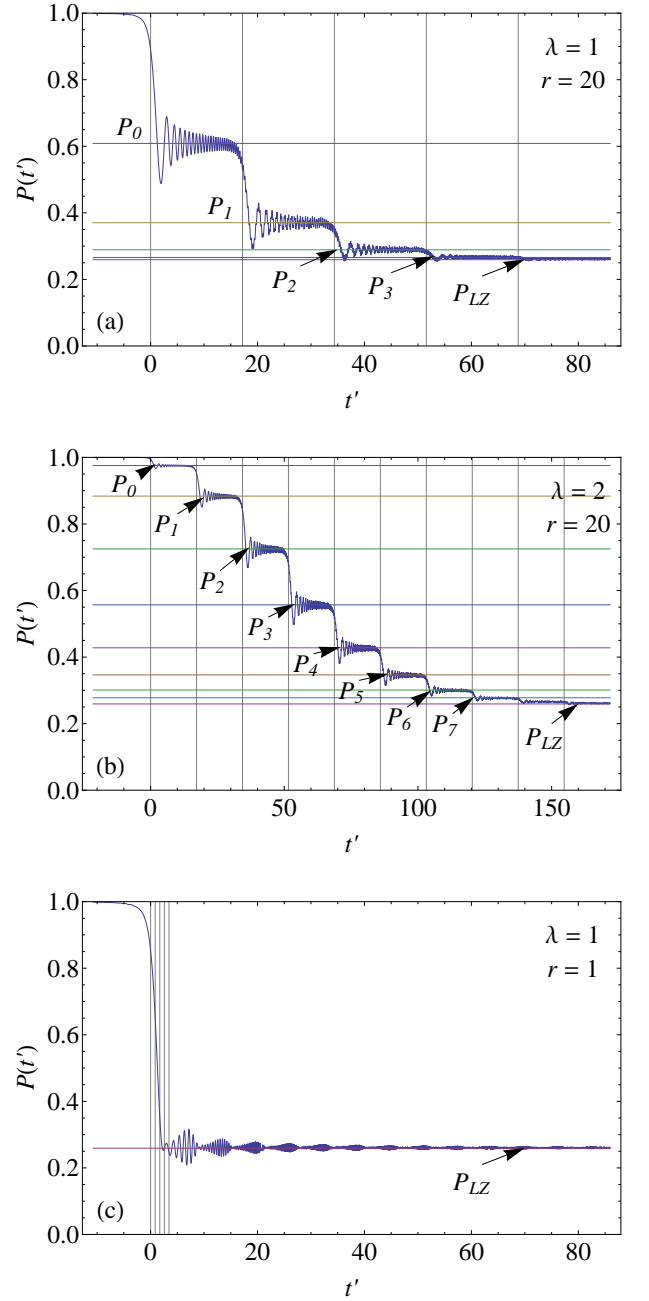


FIG. 4. Time dependence of the probability that the spin stays in the initial spin-down state for initial state $\Psi(-\infty) = |0\rangle|\downarrow\rangle$ with $\epsilon = 1.35$. Vertical lines at t_k denote avoided crossing of adiabatic energy levels. Horizontal lines are exact results P_N for independent transitions.

When the system is initially in the $|0\rangle|\downarrow\rangle$ state, all diabatic crossings will occur between energies $E_{0\downarrow}$ and $E_{n\uparrow}$. The transition probability $P_{0n} = e^{-\epsilon_{0n}}$ at each crossing depends on $|\kappa_{0n}|^2$. Using $L_0^n(x) = 1$ we obtain

$$\epsilon_{0n} = \frac{\pi \Delta^2 e^{-\lambda^2}}{2\hbar v} \frac{\lambda^{2n}}{n!}. \quad (30)$$

After the first avoided crossing at $t_0 = 0$, the asymptotic

staying probability in the initial state is $P_{00} = e^{-\epsilon_{00}}$. The next avoided crossing occurs at t_1 , and the probability of staying in the spin down state after t_1 is $P_{01} = e^{-\epsilon_{01}}$. Thus the total staying probability after two avoided crossings is $P_{00}P_{01}$. We define P_N as the probability of remaining in the initial state after N avoided crossings,

$$P_N = \exp\left(-\sum_{n=0}^N \epsilon_{0n}\right). \quad (31)$$

In the limit $N \rightarrow \infty$, we recover the exact Landau Zener probability P_{LZ} ,

$$\lim_{N \rightarrow \infty} P_N = \exp\left(-\frac{\pi \Delta^2 e^{-\lambda^2}}{2\hbar v} \sum_{n=0}^{\infty} \frac{\lambda^{2n}}{n!}\right) = \exp\left(-\frac{\pi \Delta^2}{2\hbar v}\right). \quad (32)$$

Fig. 4b shows staying probability for larger coupling, $\lambda = 2$. We see that as the tunnel splitting at each avoided crossing is more strongly renormalized, it takes more crossings to reach the final Landau-Zener probability.

As the oscillator frequency decreases compared to the sweep rate, $r \gtrsim 1$, the transitions are no longer completely independent, although small oscillations about individual plateaus can still be seen in $P(t)$. This is because the transitions happen within a small multiple of the Landau-Zener tunneling time τ_{LZ} . When the oscillator frequency and tunnel splitting are close to resonance $r \sim 1$, the transition probability initially approaches P_{LZ} and then shows collapse and revival behavior around this limit, as shown in Fig. 4c. For $r \ll 1$ the revivals become much weaker and the probability resembles the traditional LZ probability.

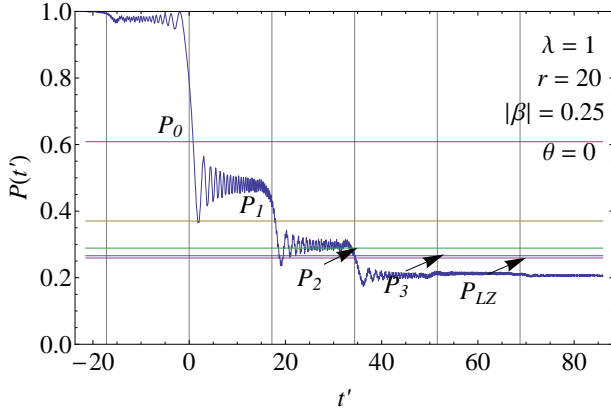


FIG. 5. Time dependence of the probability that the spin stays in the initial spin-down state for an initial coherent oscillator state $\Psi(-\infty) = |\beta\rangle|\downarrow\rangle$ with $\epsilon = 1.35$. Vertical lines at t_k denote avoided crossing of adiabatic energy levels. Horizontal lines are exact results P_N for independent transitions when starting in the $|0\rangle|\downarrow\rangle$ state.

When the oscillator is initially in a coherent state $|\beta\rangle$,

$$\Psi(-\infty) = |\beta\rangle|\downarrow\rangle = e^{-|\beta|^2/2} \sum_{n=0}^{\infty} \frac{\beta^n}{\sqrt{n!}} |n\rangle|\downarrow\rangle \quad (33)$$

where the complex number $\beta = |\beta|e^{i\theta}$ is proportional to the amplitude of initial oscillations. When $\beta \ll 1$ the spin transitions follow approximately the same asymptotic values P_N as the quantum ground state case. For $\beta \lesssim 1$ the staying probabilities, an example of which is shown in Fig. 5, depend on the magnitude and phase of the initial coherent state. The maximum angular displacement and velocity of a coherent state are related to β through

$$\varphi_{\max} = 2\lambda|\beta|, \quad \left(\frac{d\varphi}{dt'}\right)_{\max} = 2r\lambda|\beta|, \quad (34)$$

where $\varphi = 2S\langle\phi\rangle$.

C. Weak coupling

When the spin dynamics of the nanomagnet are weakly coupled to its rotational dynamics $\lambda \ll 1$, there is little observable effect of rotations on spin flip probability. The first crossing that occurs at $t_0 = 0$ has tunnel splitting $\Delta_{00} = \Delta e^{-\lambda^2/2}$, which tends to unity for small λ . When $r \gg 1$ the first transition at $t_0 = 0$ approaches $P_{00} = e^{-\epsilon_{00}}$. The second independent transition occurs at t_1 approaches P_{LZ} , although the difference between P_{00} and P_{LZ} is very small. When $r \sim 1$ the adiabatic transitions are no longer independent, and occur close to the Landau-Zener tunneling time interval.

IV. OSCILLATOR DYNAMICS

We compute the expectation value of the torsional rotation angle as a function of time

$$\varphi = \lambda \sum_{m,\sigma} (C_{m+1,\sigma}^* C_{m,\sigma} \sqrt{m+1} + C_{m-1,\sigma}^* C_{m,\sigma} \sqrt{m}). \quad (35)$$

For strong coupling $\lambda \sim 1$, the dynamics of the resonator shows a delay before the onset of large oscillations for $r \gg 1$, which occurs at t_1 , shown in Fig. 6a. When the coupling is stronger, Fig. 6b shows many more changes in the oscillatory motion, consistent with more avoided crossings. The oscillation amplitude changes slightly at subsequent t_k . As r decreases towards 1, the interval of large oscillations becomes shorter. When $r \lesssim 1$, there is a single transition region which gives way to harmonic oscillations, shown in Fig. 6c. Near $r = 1$, the amplitude of oscillations tends to increase as r decreases for fixed λ .

The angular displacement of the torsional resonator also shows interesting effects even for small coupling. When $r \gg 1$, large torsional oscillations do not begin at the first crossing. This can be understood as follows. The $t = 0$ crossing occurs between spin up and down states, both of which correspond to the ground state of

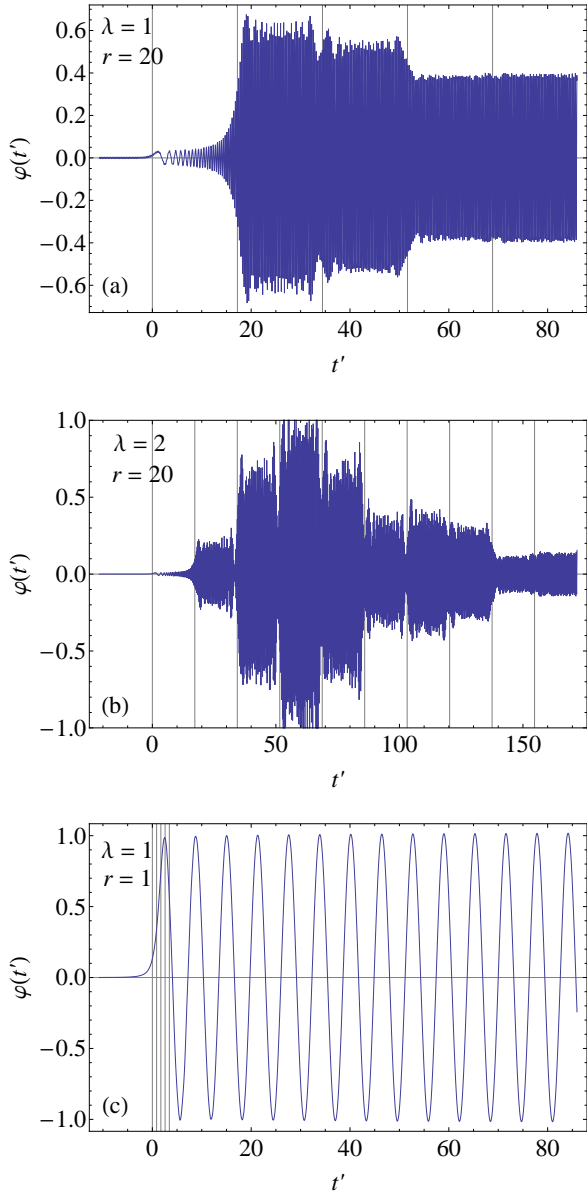


FIG. 6. Time dependence of the rotation angle expectation value for initial state $\Psi(-\infty) = |0\rangle|\downarrow\rangle$ with $\epsilon = 1.35$. Vertical lines at t_k denote avoided crossing of adiabatic energy levels.

the resonator. Although there is a small increase in displacement angle at this crossing, the largest increase occurs at the second crossing between $|0\rangle|\downarrow\rangle$ and $|1\rangle|\uparrow\rangle$ at t_1 . This delay agrees exactly with the semiclassical treatment by Jaafar et al.¹⁹. Following this time the oscillator is in a superposition of ground and excited states. When $r \lesssim 1$ successive transitions occur in a short duration compared to τ_{LZ} , and there is no observable delay in the onset of oscillations. The oscillation amplitude depends on the sweep rate. Numerical results suggest that the largest amplitude oscillation reaches a maximum near $\epsilon \simeq 2$ for $\lambda = 1$ and $r = 20$.

When the oscillator is initially in a coherent state $|\beta\rangle$,

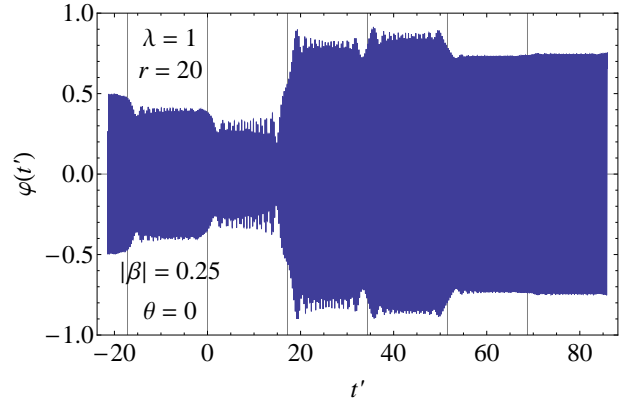


FIG. 7. Time dependence of the rotation angle expectation value for initial coherent state $\Psi(-\infty) = |\beta\rangle|\downarrow\rangle$ with $\epsilon = 1.35$. Vertical lines at t_k denote avoided crossing of adiabatic energy levels.

normal oscillations with maximum amplitude $\varphi_{\max} = 2\lambda|\beta|$ occur up to t_{-1} , as shown in Fig. 7. At t_{-1} the amplitude decreases slightly and decreases again at t_0 . A large increase occurs at t_1 , similar to the case where the oscillator is initially in its quantum ground state. The amplitude of oscillations after t_1 tends to be larger when the oscillator is initially in a coherent state, but not by a large amount. We observe a subsequent change in oscillation amplitude at t_2 and t_3 . The oscillator dynamics are not as sensitive to the initial phase of the coherent state as the spin dynamics, although there is some variation in maximum amplitude.

V. COLLECTIVE DYNAMICS OF SPINS COUPLED TO A MECHANICAL RESONATOR

Consider, instead of a single nanomagnet, an array of single molecule magnets with their easy axes mutually aligned with the axis of rotation of the resonator. If they are far enough apart that dipolar coupling is negligible, they will only be coupled through the effective field due to torsional oscillations. Because the angular displacement is the same for each molecule, this results in collective coherent dynamics, described by a variant of the Dicke Hamiltonian. For N single molecule magnets, we define the operator of total low-energy dynamics as

$$\hat{H}_R = -\frac{\Delta}{2}R_x, \quad \mathbf{R} = \sum_{i=1}^N \boldsymbol{\sigma}^i \quad (36)$$

where the index i labels each magnetic particle. Again transforming to the lab frame by performing a rotation by angle ϕ to the lab frame, but now using the total spin,

we obtain

$$\begin{aligned}\hat{H}'_R &= -\frac{\Delta}{2} (e^{-2iS\phi} R_+ + e^{2iS\phi} R_-) \\ &= -\frac{\Delta}{2} (\cos(2S\phi) R_x + \sin(2S\phi) R_y).\end{aligned}\quad (37)$$

The full Hamiltonian for the array of single molecule magnets is

$$\begin{aligned}\hat{H}_{SR} &= \frac{\hbar^2 L_z^2}{2I_z} + \frac{I_z \omega_r^2 \phi^2}{2} - \frac{W(t)}{2} R_z \\ &\quad - \frac{\Delta}{2} (\cos(2S\phi) R_x + \sin(2S\phi) R_y),\end{aligned}\quad (38)$$

where $W(t) = vt$. The Hamiltonian can be written as

$$\hat{H}_{SR} = \hat{H}_{\text{osc}} - \frac{1}{2} \mathbf{H}_{\text{eff}} \cdot \mathbf{R}, \quad (39)$$

where \hat{H}_{osc} is the uncoupled oscillator Hamiltonian and

$$\mathbf{H}_{\text{eff}} = -\frac{\delta \hat{H}}{\delta \mathbf{R}} = \Delta \cos(2S\phi) \mathbf{e}_x + \Delta \sin(2S\phi) \mathbf{e}_y + W \mathbf{e}_z \quad (40)$$

is the effective magnetic field. Noticing that \hat{H}_{SR} is linear in R_x, R_y, R_z , we can see that $[\mathbf{R}^2, \hat{H}_{SR}] = 0$, so $\mathbf{R}^2 = R(R+1)$ is a conserved quantum number and \mathbf{R} behaves as a single large isospin. We are interested in the maximum value of R , $R_{\text{max}} = N/2$, which can be experimentally realized by preparing the system with a strong longitudinal magnetic field such that all spins are pointing down.

The Heisenberg equations of motion $i\hbar d\hat{A}/dt = [\hat{A}, \hat{H}]$ are

$$\hbar \dot{L}_z = -I_z \omega^2 \phi - \Delta S (\sin(2S\phi) R_x - \cos(2S\phi) R_y) \quad (41)$$

$$\dot{\phi} = \frac{\hbar L_z}{I_z} \quad (42)$$

$$\hbar \dot{R}_x = W R_y - \Delta \sin(2S\phi) R_z \quad (43)$$

$$\hbar \dot{R}_y = -W R_x + \Delta \cos(2S\phi) R_z \quad (44)$$

$$\hbar \dot{R}_z = -\Delta \cos(2S\phi) R_y + \Delta \sin(2S\phi) R_x. \quad (45)$$

The equations of motion show a few important properties. First, the time derivative of the z -component of the total angular momentum equals the elastic torque

$$\frac{d}{dt} (\hbar L_z + \hbar S R_z) = -I_z \omega^2 \phi. \quad (46)$$

If the spin-rotor system were completely uncoupled from its environment the total angular momentum, spin plus rotational, would be conserved. In the limit $\phi \rightarrow 0$, we would obtain Heisenberg equations of motion for $R_{x,y,z}$. Solving this system of equations gives the same Landau-Zener probability of spin flip as the Schrödinger picture,

discussed in Sec. II A. Second, these equations are not independent, but

$$\frac{d}{dt} \mathbf{R}^2 = 0 \quad (47)$$

which is equivalent to $\mathbf{R}^2 = \text{constant}$, which we had found as a constant of motion of the Hamiltonian. Because the length of \mathbf{R} is fixed and large in magnitude, we see that the equations of motion for \mathbf{R} are equivalent to the Landau-Lifshitz equations for a classical spin of fixed length precessing in a magnetic field. Dividing Eqs.(41)-(45) by R shows that the direction of the total spin follows the Landau-Lifshitz equation, which is mathematically equivalent to the Schrödinger equation of a spin-half particle precessing in a magnetic field,

$$\hbar \frac{d\boldsymbol{\sigma}}{dt} = \boldsymbol{\sigma} \times \mathbf{H}_{\text{eff}}, \quad \boldsymbol{\sigma} = \frac{\mathbf{R}}{R}. \quad (48)$$

The equations of motion for $R_{x,y,z}$ can be divided through by R to giving identical equations of motion for a pseudospin $\boldsymbol{\sigma} = \mathbf{R}/R$ of unit length. Substituting this into the equation of motion for ϕ and eliminating L_z gives a second order equation of motion for the dynamics of the resonator,

$$\frac{d^2 \varphi}{dt'^2} + r^2 \varphi = -\alpha R (\sin(\varphi) \sigma_x - \cos(\varphi) \sigma_y), \quad (49)$$

where $\varphi = 2S\phi$, the prime denotes derivative with respect to dimensionless time $t' = \Delta t/\hbar$, r and α are defined in Eqs. (16) and (17), respectively.

The right hand side of Eq. (49) shows that the spins exert a collective torque on the resonator. This is a simple yet meaningful result. The equation of motion is similar to the semiclassical treatment of a single spin²⁰, but with the torque on the resonator increased by a factor of R . Because the amplitude of oscillation is proportional to the number of magnetic molecules N , this can be interpreted as a signature of Dicke phonon superradiance⁴. For a simple harmonic torsional oscillator, the phonon field is the angle of displacement from equilibrium ϕ , and the driving torque is proportional to $R = N/2$.

Returning to the quantum model we see that for the case of superradiance, $\alpha \rightarrow \alpha R$, and $\lambda = \sqrt{\alpha/r}$ becomes

$$\lambda_{SR} = \sqrt{\frac{\alpha R}{r}} = \sqrt{R} \lambda \propto \sqrt{N} \lambda. \quad (50)$$

This provides a viable method of increasing the coupling in a realistic experiment, by increasing the number of individual nanomagnets on the resonator. The usual difficulty of realizing strong coupling is that reducing the moment of inertia by even two orders of magnitude has a small effect on the coupling due to the inverse quartic root dependence of the coupling on the moment of inertia.

The Heisenberg equations of motion, Eqs. (41)-(45) are operator equations which should be averaged over the

quantum state of the system. Since the spin \mathbf{R} is classical the averages decouple, such as $\langle \sin(\varphi)\sigma_x \rangle \rightarrow \langle \sin(\varphi) \rangle \langle \sigma_x \rangle$ in Eq. (49), which yields classical-like equations of motion. We solve these equations of motion numerically.

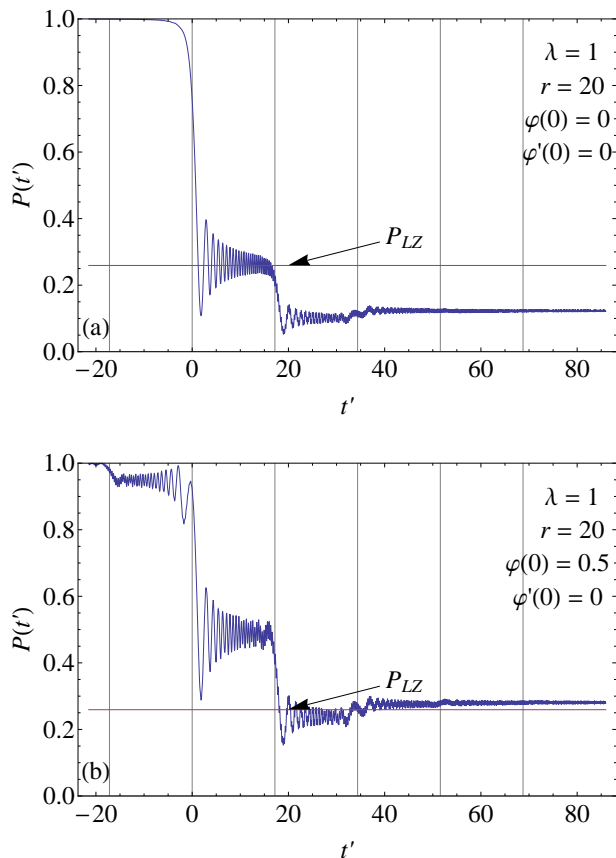


FIG. 8. Time dependence of the effective probability $P(t) = (1 - \langle \sigma_z \rangle)/2$ for the z -component of a large spin in the semiclassical model, with various initial conditions and $\epsilon = 1.35$.

We emphasize that a large spin will display the classical dynamics of a magnetic moment precessing in a time-dependent magnetic field. Plots of the probability as a function of time for the semiclassical equations of motion of a superradiant ensemble of spins are shown in Fig. 8. We see multi-stage transitions similar to the quantum case. A semiclassical explanation is as follows. Transitions occur when the energy separation between spin states equals a multiple of the oscillator frequency. These occur at the same times $t_k = r/v'$ given by Eq. (24) for the quantum case when avoided crossings between adiabatic energies occur.

When the oscillator is initially at rest at its equilibrium position $\varphi = 0$, the initial transition occurs at t_0 as shown in Fig. 8a. $P(t)$ oscillates about the regular Landau-Zener probability $P_{LZ} = e^{-\epsilon}$. Subsequent transitions occur at t_1 and t_2 , with the long-time probability much different from P_{LZ} . The spin dynamics depend strongly on the initial state of the oscillator. Fig. 8b shows the

transition probability for different initial conditions of the oscillator with the same amplitude of oscillation as the coherent state studied in the fully quantum-mechanical model.

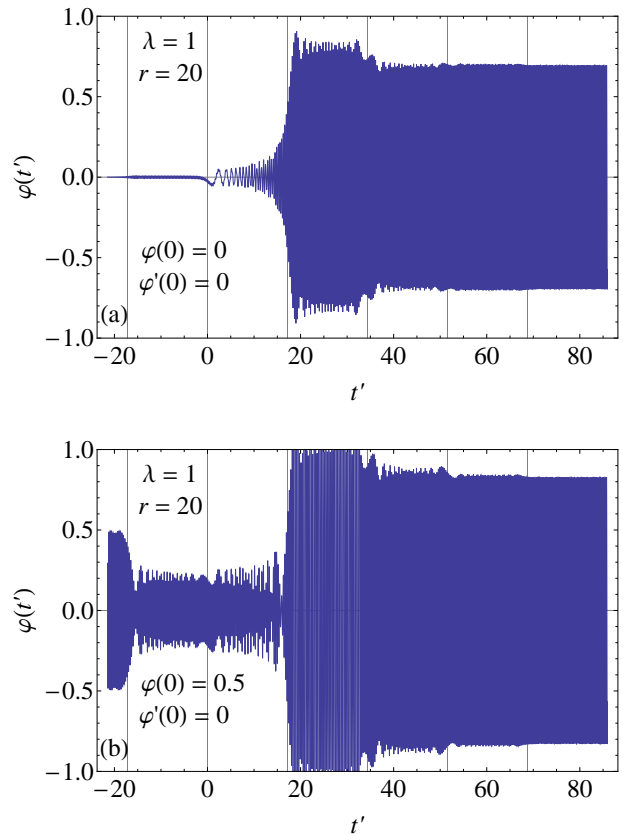


FIG. 9. Time dependence of the rotation angle in the semiclassical model, with various initial conditions and $\epsilon = 1.35$.

The oscillator dynamics show a similar delay in the onset of strong oscillations as in the quantum model, shown in Fig. 9. We notice a large increase in the amplitude of oscillations at t_1 for the cantilever initially at rest at equilibrium. For the cantilever initially oscillating with amplitude φ_0 , the behavior is very similar to the quantum model with the oscillator initially in a coherent state. We observe normal oscillations up to t_{-1} at which the amplitude decreases, then a large increase at t_1 , with subsequent changes at t_2, t_3 . While there is not a strong dependence on the initial conditions with the same initial energy, there is some variation in maximum amplitude.

VI. DISCUSSION AND CONCLUSIONS

We have studied the Landau-Zener dynamics of a tunneling spin rigidly coupled to a torsional oscillator. Starting with a quantum model describing the low energy dynamics of a tunneling macrospin, we numerically solve the time-dependent Schrödinger equation to obtain the dynamics of the expectation values of the spin and oscil-

lator. We find that when the oscillator is initially in its quantum ground state, there are a series of plateaus in the staying probability as a function of time. We analytically obtain exact probabilities in terms of tunnel splittings of the spin which are dressed by the quantum states of the torsional oscillator. These results perfectly fit the plateaus obtained from numerical simulations. The oscillator dynamics show abrupt changes in amplitude which occur at the same times as the steps between steps of the staying probability. For an oscillator initially in a coherent state we also find a stepwise staying probability curve, but these deviate from the analytical results found for the initial ground state because there are multiple occupied states of the resonator. The oscillator dynamics continue to show changes in amplitude which coincide with the steps. We also consider a large number of spins, N , on a single oscillator, and find a superradiant enhancement of the spin-oscillator coupling which scales as \sqrt{N} . As in the Dicke model, the ensemble of spins acts as a single large spin. This justifies decoupling quantum averages of separate observables in the Heisenberg equations of motion, giving semiclassical equations of motion for a large spin in a time-dependent effective field which depends on the motion of the cantilever. The cantilever experiences a harmonic restoring torque but also a driving torque due to the dynamics of the large spin. We numerically solve the set of coupled equations and compare the results to the Schrödinger picture. The spin dynamics show sensitivity to the initial state of the resonator, although the oscillator dynamics are fairly insensitive to this.

It is important to distinguish the interpretation of these results in the context of the system being measured. Consider the single molecule magnet grafted to a carbon nanotube, depicted in Fig. 1a. With the system prepared in the spin down state by a strong magnetic field along the negative z -axis, the magnetic field is swept. If the oscillator is initially in the zero phonon state, the first crossing of an occupied energy level with an unoccupied level occurs at $t_0 = 0$ between $E_{0\downarrow}$ and $E_{0\uparrow}$. $P_0 = P_{00} = e^{-\epsilon_{00}}$ is the probability that the spin will remain in the down state. If the spin remains in the down state after the first crossing, it will encounter a second crossing between $E_{0\downarrow}$ and $E_{1\uparrow}$ at t_1 , at which it will remain spin-down with probability $P_{01} = e^{-\epsilon_{01}}$. The total probability of the spin remaining spin-down after t_1 is $P_1 = P_{00}P_{01} = e^{-(\epsilon_{00}+\epsilon_{01})}$. If the spin reverses at any t_k it will see no more crossings. When the spin does reverse it will exert a torque on the carbon nanotube, exciting a phonon mode. The onset of oscillations shows that the spin has tunnelled. This provides a method of detecting the mechanical quantum state of the nanotube.

This situation is similar to the recent demonstration of electronic readout of nuclear spin states of a terbium-based single magnetic molecule²⁷. Terbium nuclear spin 3/2 has four possible projections onto the quantization axis, each projection providing a different hyperfine shift of the resonance of the Landau-Zener transition of the spin of the molecule. Time-resolved measurements show

an increase in the differential conductance at the time the spin makes a transition. This occurs at a different value of the external field for each sweep, that depends on the quantum state of the nuclear spin. In our model the role of nuclear spin states is played by the resonator states given by Eq. (23). We, therefore, propose a similar experiment in which the field sweep is used to read out the quantum state of the mechanical resonator.

When there is a large number of magnetic molecules on a cantilever, as in Fig. 1b, they will act as a single large classical spin $\mathbf{R}(t)$. This spin not only responds to the external field but also to the motion of the cantilever. The latter has been treated in Sec. V as a classical oscillator described by the angle $\phi(t)$. Such treatment is the classical limit of the quantum-mechanical consideration in which the cantilever is described by the coherent state, Eq. (33). Mechanical rotation at an angular frequency $\dot{\phi}$ is equivalent to a magnetic field $B_{\text{eff}} = \dot{\phi}/\gamma$, where γ is the gyromagnetic ratio. In turn, the spin dynamics act as a driving torque on the cantilever, resulting in coupled dynamics which change at the same moments of time, t_k , as in the quantum case. The non-linear coupled equations of motion lead to the excitations of harmonics of the cantilever that correspond to its quantum modes in the dynamics described by the Schrodinger equation. Higher harmonics are excited with smaller amplitude.

To put some of these statements into perspective, consider a spin-10 single molecule magnet grafted to a carbon nanotube²³. The moment of inertia of the magnetic molecule is of the order $I_z \sim 10^{-42} \text{ kg}\cdot\text{m}^2$. With a carbon nanotube torsional stiffness of $k \sim 10^{-18} \text{ N}\cdot\text{m}$ the simple harmonic model gives $\omega_r \sim 1000 \text{ GHz}$, which means coupling on the order of $\lambda \sim 10^{-1}$. Typical phonon frequencies of carbon nanotubes in the 10-100 GHz range would increase the coupling by an order of magnitude. Recent observation²³ of strong spin-phonon coupling in such a system estimates $\lambda \simeq 0.5$. While this is certainly large enough to observe the influence of the oscillator on spin dynamics, there is no way to directly observe oscillations in a carbon nanotube.

If the same spin-10 magnetic molecule were mounted on a paddle-shaped torsional resonator of size $20 \times 20 \times 10 \text{ nm}^3$ supported by a single carbon nanotube with torsional rigidity $k = 10^{-18} \text{ N}\cdot\text{m}$. The moment of inertia is dominated by the paddle, $I_z \sim 10^{-36} \text{ kg}\cdot\text{m}^2$, which gives $\omega_r = \sqrt{k/I_z} \sim 10^9 \text{ s}^{-1}$. The coupling parameter λ is then on the order of 10^{-2} , which would be too small to observe an effect on the spin dynamics. With $\Delta/\hbar \ll 10^9 \text{ s}^{-1}$ there should be a detectable delay between the $t = 0$ crossing and the onset of maximal oscillation amplitude. With $\Delta/\hbar > 10^9 \text{ s}^{-1}$, the delay will be undetectable. The tunnel splitting can be tuned by orders of magnitude by applying a transverse magnetic field.

A macroscopic resonator in which even small amplitude oscillations could be observed comes at the expense of weak coupling with no observable effect on the spin dynamics. In terms of the moment of inertia and torsional stiffness, the coupling goes as $\lambda \propto 1/\sqrt[4]{kI_z}$, so a

very small torsional stiffness of $k \sim 10^{-22}$ N·m would be needed. One way to overcome this limitation is to put a large number of spins on a torsional resonator or microcantilever. For a cantilever with dimensions $1000 \times 200 \times 100$ nm³ we would expect $\omega \sim 1$ GHz with $Q \sim 500$. Single molecule magnets have a diameter on the order of 1 nm. It would be possible to place hundreds of single molecule magnets on the tip of a nanocantilever separated by over 10 nm from their nearest neighbors to weaken dipolar interactions. They would act as a single large spin due to the collective quantum effect of super-radiance. This would increase the coupling by at least an

order of magnitude, as $\lambda_{SR} \propto \sqrt{N}$. Therefore it would be possible to directly observe the coupled dynamics of the magnetization and oscillatory motion in a Landau-Zener experiment.

ACKNOWLEDGMENTS

This work has been supported by the U.S. National Science Foundation through grant No. DMR-1161571.

-
- ¹ L. Landau, *Physikalische Zeitschrift der Sowjet Union* **2**, 46 (1932); C. Zener, *Proceedings of the Royal Society of London* **A137**, 7 (1932); E. Stueckelberg, *Helvetica Physica Acta* **5**, 369 (1932); E. Majorana, *Il Nuovo Cimento* (1924-1942) **9**, 43 (1932), 10.1007/BF02960953.
 - ² W. Wernsdorfer and R. Sessoli, *Science* **284**, 133 (1999).
 - ³ D. A. Garanin and R. Schilling, *Phys. Rev. B* **71**, 184414 (2005).
 - ⁴ E. M. Chudnovsky and D. A. Garanin, *Phys. Rev. Lett.* **89**, 157201 (2002); *Phys. Rev. Lett.* **93**, 257205 (2004).
 - ⁵ S. Brundobler and V. Elser, *Journal of Physics A: Mathematical and General* **26**, 1211 (1993); N. A. Sinitsyn, *Journal of Physics A: Mathematical and General* **37**, 10691 (2004).
 - ⁶ N. A. Sinitsyn, *ArXiv e-prints* (2012), arXiv:1212.2907 [cond-mat.quant-gas].
 - ⁷ W. H. Zurek, U. Dorner, and P. Zoller, *Phys. Rev. Lett.* **95**, 105701 (2005).
 - ⁸ B. Damski, *Phys. Rev. Lett.* **95**, 035701 (2005).
 - ⁹ J. Keeling and V. Gurarie, *Phys. Rev. Lett.* **101**, 033001 (2008).
 - ¹⁰ Z. Sun, J. Ma, X. Wang, and F. Nori, *Phys. Rev. A* **86**, 012107 (2012).
 - ¹¹ M. Wubs, K. Saito, S. Kohler, P. Hänggi, and Y. Kayanuma, *Phys. Rev. Lett.* **97**, 200404 (2006).
 - ¹² K. Saito, M. Wubs, S. Kohler, Y. Kayanuma, and P. Hänggi, *Phys. Rev. B* **75**, 214308 (2007).
 - ¹³ R. S. Whitney, M. Clusel, and T. Ziman, *Phys. Rev. Lett.* **107**, 210402 (2011).
 - ¹⁴ S. Shevchenko, S. Ashhab, and F. Nori, *Physics Reports* **492**, 1 (2010).
 - ¹⁵ M. LaHaye, J. Suh, P. Echternach, K. Schwab, and M. Roukes, *Nature* **459**, 960 (2009).
 - ¹⁶ T. M. Wallis, J. Moreland, and P. Kabos, *Applied Physics Letters* **89**, 122502 (2006).
 - ¹⁷ G. Zolfagharkhani, A. Gaidarzhy, P. Degiovanni, S. Kettmann, P. Fulde, and P. Mohanty, *Nat Nano* **3**, 720 (2008).
 - ¹⁸ J. P. Davis, D. Vick, J. A. J. Burgess, D. C. Fortin, P. Li, V. Sauer, W. K. Hiebert, and M. R. Freeman, *New Journal of Physics* **12**, 093033 (2010).
 - ¹⁹ R. Jaafar, E. M. Chudnovsky, and D. A. Garanin, *EPL (Europhysics Letters)* **89**, 27001 (2010).
 - ²⁰ R. Jaafar, *Journal of Magnetism and Magnetic Materials* **323**, 3151 (2011).
 - ²¹ A. A. Kovalev, L. X. Hayden, G. E. W. Bauer, and Y. Tserkovnyak, *Phys. Rev. Lett.* **106**, 147203 (2011).
 - ²² D. A. Garanin and E. M. Chudnovsky, *Phys. Rev. X* **1**, 011005 (2011).
 - ²³ M. Ganzhorn, S. Klyatskaya, M. Ruben, and W. Wernsdorfer, *Nature Nanotechnology* **advance online publication**, (2013).
 - ²⁴ E. M. Chudnovsky, *Phys. Rev. Lett.* **72**, 3433 (1994).
 - ²⁵ E. M. Chudnovsky and D. A. Garanin, *Phys. Rev. B* **81**, 214423 (2010); M. O’Keeffe, E. Chudnovsky, and D. Garanin, *Journal of Magnetism and Magnetic Materials* **324**, 2871 (2012).
 - ²⁶ D. A. Garanin, *Journal of Physics A: Mathematical and General* **24**, L61 (1991).
 - ²⁷ R. Vincent, S. Klyatskaya, M. Ruben, W. Wernsdorfer, and F. Balestro, *Nature* **488**, 357 (2012).